Inorganic Chemistry

Article

pubs.acs.org/IC

X-ray Structures of $Sc_2C_2@C_{2n}$ (n = 40–42): In-Depth Understanding of the Core–Shell Interplay in Carbide Cluster Metallofullerenes

Hiroki Kurihara,[†] Xing Lu,[†] Yuko Iiduka,[†] Hidefumi Nikawa,[†] Makoto Hachiya,[†] Naomi Mizorogi,[†] Zdenek Slanina,[†] Takahiro Tsuchiya,[†] Shigeru Nagase,*[,‡] and Takeshi Akasaka*[,†]

[†]Life Science Center of Tsukuba Advanced Research Alliance, University of Tsukuba, Tsukuba, Ibaraki 305-8577, Japan

[‡]Department of Theoretical and Computational Molecular Science, Institute for Molecular Science, Okazaki, Aichi 444-8585, Japan

Supporting Information

ABSTRACT: X-ray analyses of the cocrystals of a series of carbide cluster metallofullerenes $Sc_2C_2@C_{2n}$ (n = 40–42) with cobalt(II) octaethylporphyrin present new insights into the molecular structures and cluster–cage interactions of these less-explored species. Along with the unambiguous identification of the cage structures for the three isomers of $Sc_2C_2@C_{2v}(5)$-C_{80}, $Sc_2C_2@C_{3v}(8)$-C_{82}, and $Sc_2C_2@D_{2d}(23)$-C_{84}, a clear correlation between the cluster strain and cage size is observed in this series: Sc–Sc distances and dihedral angles of the bent cluster increase along with cage expansion, indicating that the bending strain within the cluster makes it pursue a planar structure to the greatest degree possible. However, the C–C distances within Sc_2C_2 remain unchanged when the cage expands, perhaps because of the unusual bent structure of the cluster, preventing contact between the cage and the C_2 unit. Moreover, analyses revealed that larger cages provide more space for the cluster to rotate. The preferential formation of cluster endohedral metallofullerenes for scandium might be associated with its small ionic radius and the strong coordination ability as well.

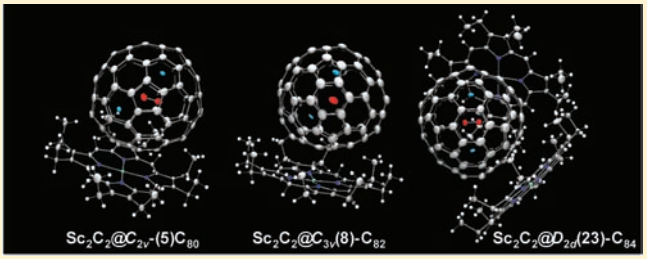

INTRODUCTION

The strategy of putting metal atoms or complexes into fullerene interiors has been attracting intensive attention along with the exohedral functionalization of fullerenes because both show great success in generating novel functional materials with vast applications in various fields such as biomedicine, photovoltaics, and electronics.[1−9] These fullerene–metal hybrid materials, called endohedral metallofullerenes (EMFs), nevertheless, have not received attention equal to that of their relatives, empty fullerenes, even though they came to human realization almost simultaneously.[10,11] Two main reasons account for these circumstances: the low production yield of EMFs and complexation of the metallic species with the cage, which makes the acquisition and characterization of EMFs fairly difficult. For example, the paramagnetism of some mono-EMFs (e.g., $La@C_{82}$) impedes direct NMR determination.[12,13]

Recently, great success has been achieved in the synthesis and isolation of some stable EMF species, which enables the complete structural characterization and further functionalization of such high-yield EMFs as $M@C_{82}$ and $M_3N@C_{80}$.[14,15] As a direct result, many useful materials based on functionalized EMFs have been generated, some of which show great promise in reality.[16−21] However, elucidation of the EMF structure persists as an intimidating challenge because of the diversity of the endohedral metallic species that can be encapsulated. To date, metallic compositions of many kinds have been found within EMFs. In addition to such species containing purely metal atoms (one or two), which are viewed as conventional EMFs, unconventional EMFs encapsulating a cluster of metal carbide ($M_2C_2/M_3C_2/M_4C_2$), nitride (M_3N), oxide ($M_2O/M_2O_3/M_3O_2/M_4O_2$), sulfide ($M_2S$), and even cyanide ($M_3CN$) are all synthesized. Most of the isolated isomers have been fully characterized using various techniques including single-crystal X-ray crystallography.[22−26]

While the formation of other cluster EMFs (nitride, cyanide, oxide, and sulfide) demands a certain amount of extra additives into the reaction chamber that supplies the nonmetal element to form the clusters, generation of carbide cluster EMFs can be achieved simply by burning a graphite rod filled with metal alloys. Consequently, carbide cluster EMFs are unique because two, and exactly two, C atoms can be encapsulated inside the cage cavity along with several metal atoms. Accordingly, the structural elucidation of carbide cluster EMFs is extremely difficult; actually, many have been wrongly assigned in previous studies as conventional EMFs.[27−32]

The carbide content in EMFs was recognized[27] in 1999. In that study, the molecular structure of $Sc_2C_2@D_{2d}(23)$-C_{84}, instead of $Sc_2@C_{86}$, was proposed according to both NMR results and the maximum entropy method coupled with Rietveld treatment of synchrotron powder X-ray diffraction data (PXRD/Rietveld/MEM). However, they incorrectly assigned the signal from the internal C_2 unit (92 ppm).[27] Moreover, the NMR technique presents barely sufficient

Received: November 13, 2011
Published: December 9, 2011

Table 1. Crystallographic Data of $Sc_2C_2@C_{2n}$/Co(OEP)

	$Sc_2C_2@C_{2v}(5)$-C_{80}·Co(OEP)·2$CHCl_3$	$Sc_2C_2@C_{3v}(8)$-C_{82}·Co(OEP)·2$CHCl_3$	$Sc_2C_2@D_{2d}(23)$-C_{84}·[Co(OEP)]$_2$·2.5$CHCl_3$·CS_2
T, K	90(2)	90(2)	90(2)
λ, Å	0.710 73	0.710 73	0.710 75
color/habit	black/block	black/block	black/block
cryst size, mm	0.40 × 0.25 × 0.21	0.27 × 0.18 × 0.16	0.36 × 0.33 × 0.30
empirical formula	$C_{120}H_{46}Cl_6CoN_4Sc_2$	$C_{122}H_{46}Cl_6CoN_4Sc_2$	$C_{161.5}H_{90.5}Cl_{7.5}Co_2N_8S_2Sc_2$
fw	1905.16	1929.17	2680.69
cryst syst	monoclinic	monoclinic	triclinic
space group	$C2$	$C2$	$P\bar{1}$
a, Å	25.2029(5)	25.0092(4)	14.7682(19)
b, Å	15.2891(3)	15.4199(3)	14.815(2)
c, Å	19.2077(4)	19.3935(3)	26.657(3)
α, deg	90	90	86.286(6)
β, deg	93.5530(10)	93.1030(10)	88.601(5)
γ, deg	90	90	73.357(6)
V, Å^3	7387.1(3)	7467.9(2)	5576.1(13)
Z	4	4	2
ρ, g/cm^3	1.713	1.716	1.595
μ, mm^{-1}	0.687	0.681	0.694
R1 (obsd data)	0.054	0.0602	0.0798
R1 (all data)	0.0645	0.0828	0.0924
wR2 (obsd data)	0.149	0.1585	0.2162
wR2 (all data)	0.1612	0.1792	0.2279

information related to the cluster position and orientation, as well as metal−cage interaction, whereas the PXRD/Rietveld/MEM method is unauthentic, so that the single-crystal X-ray diffraction (XRD) method has become the final solution for EMF structures.

With concrete single-crystal XRD results, several Sc-containing EMFs have been found to bear carbide structures but all had been proposed as conventional EMFs in previous studies.[33−35] For example, the longstanding $Sc_3@C_{3v}(7)$-C_{82} proposed by the PXRD/MEM/Rietveld method, as well as the previously assigned $Sc_2@C_{82}$ and $Sc_2@C_{84}$ isomers with NMR techniques, was determined to be a carbide EMF with unambiguous single-crystal XRD measurements.[28−32] To get good crystals, the EMFs were chemically modified to hinder the free rotation of the spherical molecules in the crystal. However, because an addend (or more) is attached to the cage surface, both the cage structure and the cluster conformation are thus different from those in pristine EMFs.[9] It was recently revealed that framework rearrangement occurs on fullerenes upon chemical modification. For example, the isolated pentagon rule (IPR)-obeying D_2-C_{76} rearranges to a non-IPR isomer upon chlorination.[36] Accordingly, functionalized EMFs may have a situation for the internal metals and possibly the cage structure different from that of pristine EMFs. Therefore, obtaining the X-ray structure of unmodified EMFs is still necessary for elucidation of their properties and formation origins.

Another effective strategy of obtaining good single crystals of EMFs is complexation with metal porphyrins, which seems a bit advantageous over the chemical modification method as the structural issues of "pristine" EMFs are retained in cocrystals because of the weak interactions between the EMF molecule and metal porphyrin. This strategy has shown great success in XRD structural characterization of EMFs. Many earlier studies have specifically examined conventional EMFs and metal nitride EMFs.[37−42] The only example of metal carbide cluster EMF that has been determined structurally using single-crystal XRD measurement performed on its cocrystal with metal porphyrin is $Gd_2C_2@D_3(85)$-C_{92}. Although disorder exists, it is conclusive from the X-ray data that the cluster prefers a flat configuration within the cage. More interestingly, results show that the C−C distance of the Gd_2C_2 cluster is extraordinarily short, 1.04 Å, which is sufficiently interesting to attract further X-ray explorations of other carbide EMFs.[43] Nevertheless, no additional report describing X-ray structures of unsubstituted carbide cluster EMFs has been available in the literature.

This report describes the X-ray structures of a series of unfunctionalized carbide cluster EMFs with sequentially increasing cage size: $Sc_2C_2@C_{2v}(5)$-C_{80}, $Sc_2C_2@C_{3v}(8)$-C_{82}, and $Sc_2C_2@D_{2d}(23)$-C_{84}. All are cocrystallized with Co(OEP) (OEP = 2,3,7,8,12,13,17,18-octaethylporphinate). We discovered here for the first time that the cluster configuration, orientation, and motion are strongly dependent on the cage size and, probably, cage symmetry.

EXPERIMENTAL SECTION

The EMFs studied here were synthesized using an improved arc-discharge method and isolated with multiple-stage high-performance liquid chromatography (HPLC) separations. The purity of all samples was estimated as higher than 99% with both HPLC analysis and laser desorption time-of-flight mass spectrometry. The characteristic visible−near-IR (NIR) spectra of isolated $Sc_2C_2@C_{2n}$ isomers are shown in Figure S1 in the Supporting Information.

Cocrystals were obtained by layering a saturated chloroform solution of Co(OEP) over a concentrated CS_2 solution of the fullerene (1 mg/mL) inside a glass tube (diameter 7 mm). Over 10−14 days, the two solutions diffused together and black crystals formed on the wall and at the bottom of the tube. X-ray data of the C_{80} and C_{82} systems were collected at 90 K with a diffractometer (APEX II; Bruker Analytik GmbH) equipped with a CCD collector, whereas that of $Sc_2C_2@C_{84}$ was collected using a different device (R-AXISIP; Rigaku Corp.). Numerical methods were used for absorption correction. Direct methods were used to solve the structures.

Table 1 presents the crystal data of the cocrystals under study. The crystals of the two small cages (C_{80} and C_{82} systems) fall into the monoclinic $C2$ space group, which contains an intact fullerene sphere

dx.doi.org/10.1021/ic202438u | Inorg. Chem. 2012, 51, 746−750

and its contents (both disordered) and a complete Co(OEP) molecule (perfectly ordered). This presents an advantage over the monoclinic $C2/m$ space group, which has been encountered frequently in previous studies of the cocrystals of EMFs/M(OEP) (M = Ni or Co).[37−42] In the latter, only half the fullerene sphere and half M(OEP) are present in the crystal unit. In most cases, two cage orientations can be picked up. Because no symmetry element of the cage coincides with the crystallographic mirror plane, an intact cage can only be obtained by combining one cage orientation with the mirror image of the other one, assuming half-occupancy for each, and the complete molecule must be refined as a rigid object. Accordingly, the obtained structure might deviate slightly from the true situation because many structural restraints are applied. The space group of the C_{84} system is triclinic $P\bar{1}$, which includes a whole cage but two complete Co(OEP) molecules. This also allows accurate estimation of the cage structure and the cluster disorder.[41] More details are discussed in the following text.

RESULTS AND DISCUSSION

Figure 1 portrays the molecular structure of $Sc_2C_2@C_{2v}(5)$-C_{80} and its relation to Co(OEP). A relatively flat region of the fullerene interacts with the metal porphyrin. The nearest Co−cage distances are 2.67 and 2.69 Å, respectively, for sites 1 and 2 (Table 1), similar to the values reported for other fullerenes in the cocrystals with Co(OEP), featuring $\pi-\pi$ interactions.[37−42] Disorder exists for the cage and its content. Two cage orientations with equal occupancy are detectable along with two Sc_2C_2 configurations. Because of their matching occupancy, it can be reasonably assumed that one cage orientation pairs one cluster disorder. Only one cage and the major Sc_2C_2 site with 0.53 occupancy is shown in Figure 1 for clarity. The cluster is bent like a butterfly with two tightly bonded C atoms in the cage center. The two Sc atoms lie between the C_2 unit and the cage. The Sc−Sc distances in both pairs are 4.31 Å, and the Sc−C_2−Sc dihedral angles are 131° and 127° for sites 1 and 2, respectively, confirming a high torsion within the cluster. The average C−C distance of the cluster is 1.20 Å, which represents a typical C≡C triple bond, but this value is obviously longer than that observed in $Gd_2C_2@C_{92}$ (1.04 Å).[43] The local environments of the two Sc atoms differ: one approaches a hexagonal ring, whereas the other is near a [6,6] bond. The shortest Sc−cage contacts of the two Sc atoms in both sites are similar, ranging from 2.19 to 2.23 Å. Results show that the internal cluster is fixed inside the cage, which is consistent with previous NMR results showing that the cluster motion is highly temperature-dependent.[32]

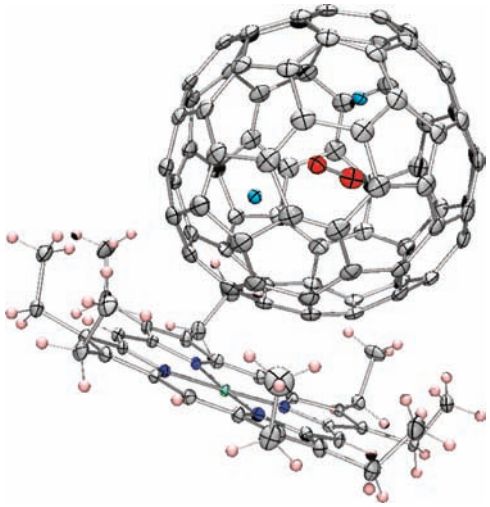

Figure 1. Perspective view of the fullerene and Co^{II}(OEP) molecules in $Sc_2C_2@C_{2v}(5)$-C_{80}·Co(OEP)·$2CHCl_3$ showing 50% thermal contours. For clarity, solvent molecules are omitted and only one carbon cage and the major Sc_2C_2 site are shown.

The crystal structure of $Sc_2C_2@C_{3v}(8)$-C_{82} also includes two cage orientations but seven Sc positions; six of them can be paired into three sets according to their stereo locations and similar occupancies (Table 2 and Figure S3 in the Supporting Information). These correspond to an oscillating cluster inside the cage. Figure 2 depicts the major cage encapsulating the major Sc_2C_2 cluster along with the pairing Co(OEP) molecule showing their spatial relationship. Again the part of the fullerene cage interacting with the plane of Co(OEP) is relatively flat. The nearest Co−cage distances are 2.78 and 2.81 Å for the two sites, markedly longer than the values in the C_{80} system. Although the dihedral angles (132° and 128° for sites 1 and 2, respectively) of the major cluster orientations are comparable to these of the C_{80} system, the Sc−Sc distances (3.86 and 3.98 Å) are slightly shorter, indicating that the cluster is more compact. Nevertheless, the C−C distances of the

Table 2. Selected Interatomic Distances and Angles

		$Sc_2C_2@C_{2v}(5)$-C_{80}·Co(OEP)·$2CHCl_3$		$Sc_2C_2@C_{3v}(8)$-C_{82}·Co(OEP)·$2CHCl_3$			$Sc_2C_2@D_{2d}(23)$-C_{84}·$[Co(OEP)]_2$·$2.5CHCl_3$·CS_2			
		site 1	site 2	site 1	site 2	site 3	site 1	site 2	site 3	site 4
occupancy	cage	0.5	0.5	0.53	0.47		1			
	C_2 unit	0.5	0.5	0.5	0.5		0.4	0.3	0.3	
	Sc	0.47	0.53	0.62 (Sc1A)	0.26 (Sc2A)	0.11 (Sc3A)	0.71	0.2	0.05	0.04
				0.52 (Sc1B)	0.32 (Sc2B)	0.07 (Sc3B)				
shortest Co−cage		2.67(1)	2.69(1)	2.78(2)	2.81(2)		2.785(4), 2.833(4)			
C−C		1.197(7)	1.196(9)	1.19(1)	1.20(2)		1.20(1)	1.20(1)	1.20(1)	
Sc−Sc		4.312(3)	4.312(3)	3.981(4)	3.86(1)	4.09(3)	4.468(9)	4.435(5)	4.47(2)	4.43(2)
Sc−C_2−Sc dihedral angle		130.8(3)	127.0(3)	132.5(4)	127.9(6)	145(1)	150.2(5)	151.7(6)	154.3(7)	149.4(8)
shortest Sc−cage		2.20(1) 2.23(1)	2.19(2) 2.19(1)	2.18(2) 2.20(2)	2.18(2) 2.22(2)	1.99(2), 2.10(3)	2.215(4) 2.182(4)	1.862(6) 2.079(5)	1.99(1) 2.02(1)	2.01(1) 2.01(2)

dx.doi.org/10.1021/ic202438u | Inorg. Chem. 2012, 51, 746−750

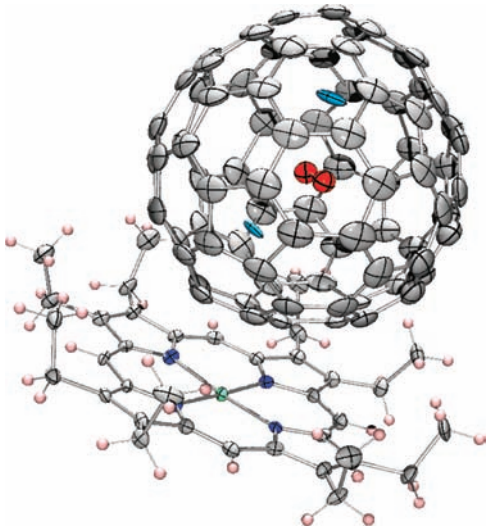

Figure 2. Perspective view of the fullerene and $Co^{II}(OEP)$ molecules in $Sc_2C_2@C_{3v}(8)$-C_{82}·Co(OEP)·2$CHCl_3$ showing 50% thermal contours. For clarity, solvent molecules are omitted and only one carbon cage and the major Sc_2C_2 site are shown.

cluster (1.19−1.20 Å) and the shortest Sc−cage contacts (1.99−2.22 Å) are not changed much.

As Figure 3 shows, the crystal of $Sc_2C_2@D_{2d}(23)$-C_{84}·[Co(OEP)]$_2$·2.5$CHCl_3$·CS_2 is distinctive.[42] It contains one

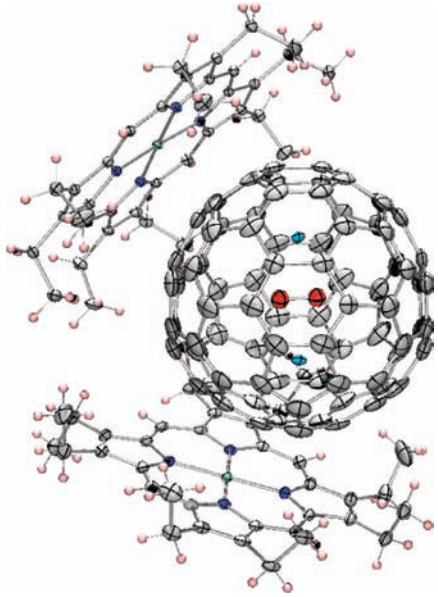

Figure 3. Perspective view of the fullerene and $Co^{II}(OEP)$ molecules in $Sc_2C_2@D_{2d}(23)$-C_{84}·[Co(OEP)]$_2$·2.5$CHCl_3$·CS_2 showing 50% thermal contours. For clarity, solvent molecules are omitted and only one carbon cage and the major Sc_2C_2 site are shown.

endohedral but two Co(OEP) molecules, which are nearly perpendicular to each other. This might originate from the high cage symmetry, which makes the cage "rounder" than the two smaller cages so that no "flat" region can specifically interact with Co(OEP). The nearest Co−cage distances are 2.78 and 2.83 Å, respectively, slightly longer than the values in the smaller cage systems. Accordingly, the correlation between the Co−cage distance and cage size in the series under study is distinguishable: the larger the cage, the longer the distance. Four pairs of Sc sites are distinguishable from the X-ray data together with three C_2 pairs, indicating a rotating cluster. Because of the asymmetric occupancy values between Sc positions and C_2-unit orientations, it is hard to pair one to the other. This situation indicates that rotation of the two Sc atoms is independent of the C_2 unit. Only the major Sc positions (0.71 occupancy) and the most abundant C_2 unit (0.4 occupancy) are shown in Figure 3. In this configuration, the Sc_2C_2 cluster is more planar than those in the smaller C_{80} and C_{82} cages with a dihedral angle of 149.4−154.3°. Similarly, the Sc−Sc distances are also longer than those of the previous two smaller systems.

Structural data of the three endohedrals are presented in Table 2. An interesting feature is observed in this series. Although no disorder of the cluster relative to cage is found in the C_{80} system, the metals are more likely to move inside the C_{82} cage because more than three pairs of Sc positions are distinguished. In the C_{84} system, four disordered metal positions and three C_2 unit positions are observed, clearly indicating a rotating cluster (Figures S2−S4, Supporting Information). It is therefore reasonable to conclude that the cage size is an important factor dictating the cluster motion, but the effect of cage symmetry (shape) seems also sound. Furthermore, the bent cluster prefers a planar structure to the greatest degree possible, which results in an increase of the Sc−Sc distances and dihedral angles along with cage expansion. However, the C−C bond length of the C_2 unit remains unchanged when the cage size increases. This is most probably because of the highly strained bent cluster, preventing the C_2 unit from interacting with the cage.

CONCLUSION

In summary, we have obtained a series of carbide cluster EMFs with sequentially increasing cage sizes: $Sc_2C_2@C_{2v}(5)$-C_{80}, $Sc_2C_2@C_{3v}(8)$-C_{82}, and $Sc_2C_2@D_{2d}(23)$-C_{84}. X-ray examination of their cocrystals with Co(OEP) revealed that the Sc_2C_2 cluster tends to pursue a planar structure to the greatest degree possible, as reflected by the increasing Sc−Sc distances and Sc−C_2−Sc dihedral angles with the cage size. However, the C−C distances within the carbide cluster remain constant upon cage expansion, indicating that the C_2 unit is important for stabilization of the entire cluster. Moreover, the cluster motion is strongly dependent on the cage size: it is nearly fixed in C_{80} but oscillates inside C_{82} and rotates in C_{84}. The dictation of cluster orientation and motion by the cage size and symmetry is firmly revealed in our study, which has presented new insights into the structure of carbide cluster EMFs. It is expected that future theoretical calculations based on our solid results will elucidate more information related to the physicochemical properties and formation mechanism of such less-explored EMFs.

ASSOCIATED CONTENT

Supporting Information

Visible−NIR spectra and X-ray data of $Sc_2C_2@C_{2n}$ (n = 40−42). This material is available free of charge via the Internet at http://pubs.acs.org.

AUTHOR INFORMATION

Corresponding Author

*E-mail: akasaka@tara.tsukuba.ac.jp (T.A.), nagase@ims.ac.jp (S.N.).

■ ACKNOWLEDGMENTS

This work is supported, in part, by a Grant-in-Aid for Scientific Research on Innovative Areas (Grant 20108001, "π-Space"), a Grant-in-Aid for Scientific Research (A) (Grant 20245006), The Next Generation Super Computing Project (Nanoscience Project), Nanotechnology Support Project, and Grants-in-Aid for Scientific Research on Priority Area (Grants 20036008 and 20038007) and Specially Promoted Research (Grant 22000009) from the Ministry of Education, Culture, Sports, Science, and Technology of Japan. H.K. thanks the Japan Society for the Promotion of Science for the Research Fellowship for Young Scientists.

■ REFERENCES

(1) Endofullerenes: *A New Family of Carbon Clusters*; Akasaka, T., Nagase, S., Eds.; Kluwer: Dordrecht, The Netherlands, 2002.
(2) *Chemistry of Nanocarbons*; Akasaka, T., Wudl, F., Nagase, S., Eds.; John Wiley & Sons: Chichester, 2010.
(3) Lu, X.; Akasaka, T.; Nagase, S. Rare Earth Metals Trapped inside Fullerenes− Endohedral Metallofullerenes. In *Rare Earth Coordination Chemistry: Fundamentals and Applications*; Huang, C. H., Ed.; John Wiley & Sons: Singapore, 2010; pp 273−308.
(4) Dunsch, L.; Yang, S. *Small* **2007**, *3*, 1298−1320.
(5) Chaur, M. N.; Melin, F.; Ortiz, A. L.; Echegoyen, L. *Angew. Chem., Int. Ed.* **2009**, *48*, 7514−7538.
(6) Yamada, M.; Akasaka, T.; Nagase, S. *Acc. Chem. Res.* **2010**, *43*, 92−102.
(7) Rodríguez-Fortea, A.; Balch, A. L.; Poblet, J. M. *Chem. Soc. Rev.* **2011**, *40*, 3551−3563.
(8) Maeda, Y.; Tsuchiya, T.; Lu, X.; Takano, Y.; Akasaka, T.; Nagase, S. *Nanoscale* **2011**, *3*, 2421−2429.
(9) Lu, X.; Akasaka, T.; Nagase, S. *Chem. Commun.* **2011**, *47*, 5942−5957.
(10) Kroto, H. W.; Heath, J. R.; Obrien, S. C.; Curl, R. F.; Smalley, R. E. *Nature* **1985**, *318*, 162−163.
(11) Heath, J. R.; Obrien, S. C.; Zhang, Q.; Liu, Y.; Curl, R. F.; Kroto, H. W.; Tittel, F. K.; Smalley, R. E. *J. Am. Chem. Soc.* **1985**, *107*, 7779−7780.
(12) Akasaka, T.; Wakahara, S.; Nagase, K.; Kobayashi, M.; Waelchli, K.; Yamamoto, M.; Kondo, S.; Shirakura, S.; Okubo, Y.; Maeda, T.; Kato, M.; Kako, Y.; Nakadaira, R.; Nagahata, X.; Gao, E.; Van Caemelbecke, K. M.; Kadish, K. M. *J. Am. Chem. Soc.* **2000**, *122*, 9316−9317.
(13) Wakahara, T.; Kobayashi, J.; Yamada, M.; Maeda, Y.; Tsuchiya, T.; Okamura, M.; Akasaka, T.; Waelchli, M.; Kobayashi, K.; Nagase, S.; Kato, T.; Kako, M.; Yamamoto, K.; Kadish, K. M. *J. Am. Chem. Soc.* **2004**, *126*, 4883−4887.
(14) Stevenson, S.; Rice, G.; Glass, T.; Harich, K.; Cromer, F.; Jordan, M. R.; Craft, J.; Hadju, E.; Bible, R.; Olmstead, M. M.; Maitra, K.; Fisher, A. J.; Balch, A. L.; Dorn, H. C. *Nature* **1999**, *401*, 55−57.
(15) (a) Yang, S. F.; Dunsch, L. *Chem.—Eur. J.* **2006**, *12*, 413−419. (b) Lu, X.; Nikawa, H.; Feng, L.; Tsuchiya, T.; Maeda, Y.; Akasaka, T.; Mizorogi, N.; Slanina, Z.; Nagase, S. *J. Am. Chem. Soc.* **2009**, *131*, 12066−12067.
(16) Iezzi, E. B.; Duchamp, J. C.; Fletcher, K. R.; Glass, T. E.; Dorn, H. C. *Nano Lett.* **2002**, *2*, 1187−1190.
(17) Bolskar, R. D. *Nanomedicine* **2008**, *3*, 201−213.
(18) Pinzon, J. R.; Gasca, D. C.; Sankaranarayanan, S. G.; Bottari, G.; Torres, T.; Guldi, D. M.; Echegoyen, L. *J. Am. Chem. Soc.* **2009**, *131*, 7727−7734.
(19) Takano, Y.; Herranz, M. A.; Martin, N.; Radhakrishnan, S. G.; Guldi, D. M.; Tsuchiya, T.; Nagase, S.; Akasaka, T. *J. Am. Chem. Soc.* **2010**, *132*, 8048−8055.
(20) Guldi, D. M.; Feng, L.; Radhakrishnan, S. G.; Nikawa, H.; Yamada, M.; Mizorogi, N.; Tsuchiya, T.; Akasaka, T.; Nagase, S.; Herranz, M. A.; Martin, N. *J. Am. Chem. Soc.* **2010**, *132*, 9078−9086.
(21) Feng, L.; Radhakrishnan, S. G.; Mizorogi, N.; Slanina, Z.; Nikawa, H.; Tsuchiya, T.; Akasaka, T.; Nagase, S.; Martin, N.; Guldi, D. M. *J. Am. Chem. Soc.* **2011**, *133*, 7608−7618.
(22) Mercado, B. Q.; Beavers, C. M.; Olmstead, M. M.; Chaur, M. N.; Walker, K.; Holloway, B. C.; Echegoyen, L.; Balch, A. L. *J. Am. Chem. Soc.* **2008**, *130*, 7854−7855.
(23) Stevenson, S.; Mackey, M. A.; Stuart, M. A.; Phillips, J. P.; Easterling, M. L.; Chancellor, C. J.; Olmstead, M. M.; Balch, A. L. *J. Am. Chem. Soc.* **2008**, *130*, 11844−11845.
(24) Beavers, C. M.; Chaur, M. N.; Olmstead, M. M.; Echegoyen, L.; Balch, A. L. *J. Am. Chem. Soc.* **2009**, *131*, 11519−11524.
(25) Wang, T. S.; Feng, L.; Wu, J. Y.; Xu, W.; Xiang, J. F.; Tan, K.; Ma, Y. H.; Zheng, J. P.; Jiang, L.; Lu, X.; Shu, C. Y.; Wang, C. R. *J. Am. Chem. Soc.* **2010**, *132*, 16362−16364.
(26) Mercado, B. Q.; Chen, N.; Rodriguez-Fortea, A.; Mackey, M. A.; Stevenson, S.; Echegoyen, L.; Poblet, J. M.; Olmstead, M. M.; Balch, A. L. *J. Am. Chem. Soc.* **2011**, *133*, 6752−6760.
(27) Wang, C. R.; Kai, T.; Tomiyama, T.; Yoshida, T.; Kobayashi, Y.; Nishibori, E.; Takata, M.; Sakata, M.; Shinohara, H. *Angew. Chem., Int. Ed.* **2001**, *40*, 397−399.
(28) Iiduka, Y.; Wakahara, T.; Nakahodo, T.; Tsuchiya, T.; Sakuraba, A.; Maeda, Y.; Akasaka, T.; Yoza, K.; Horn, E.; Kato, T.; Liu, M. T. H.; Mizorogi, N.; Kobayashi, K.; Nagase, S. *J. Am. Chem. Soc.* **2005**, *127*, 12500−12501.
(29) Iiduka, Y.; Wakahara, T.; Nakajima, K.; Tsuchiya, T.; Nakahodo, T.; Maeda, Y.; Akasaka, T.; Mizorogi, N.; Nagase, S. *Chem. Commun.* **2006**, 2057−2059.
(30) Iiduka, Y.; Wakahara, T.; Nakajima, K.; Nakahodo, T.; Tsuchiya, T.; Maeda, Y.; Akasaka, T.; Yoza, K.; Liu, M. T. H.; Mizorogi, N.; Nagase, S. *Angew. Chem., Int. Ed.* **2007**, *46*, 5562−5564.
(31) Yamazaki, Y.; Nakajima, K.; Wakahara, T.; Tsuchiya, T.; Ishitsuka, M. O.; Maeda, Y.; Akasaka, T.; Waelchli, M.; Mizorogi, N.; Nagase, S. *Angew. Chem., Int. Ed.* **2008**, *47*, 7905−7908.
(32) Kurihara, H.; Lu, X.; Iiduka, Y.; Mizorogi, N.; Slanina, Z.; Tsuchiya, T.; Akasaka, T.; Nagase, S. *J. Am. Chem. Soc.* **2011**, *133*, 2382−2385.
(33) Takata, M.; Nishibori, E.; Umeda, B.; Sakata, M.; Yamamoto, E.; Shinohara, H. *Phys. Rev. Lett.* **1997**, *78*, 3330−3333.
(34) Takata, M.; Nishibori, E.; Sakata, M.; Inakuma, M.; Yamamoto, E.; Shinohara, H. *Phys. Rev. Lett.* **1999**, *83*, 2214−2217.
(35) Inakuma, M.; Yamamoto, E.; Kai, T.; Wang, C. R.; Tomiyama, T.; Shinohara, H.; Dennis, T. J. S.; Hulman, M.; Krause, M.; Kuzmany, H. *J. Phys. Chem. B* **2000**, *104*, 5072−5077.
(36) Ioffe, I. N.; Goryunkov, A. A.; Tamm, N. B.; Sidorov, L. N.; Kemnitz, E.; Troyanov, S. I. *Angew. Chem., Int. Ed.* **2009**, *48*, 5904−5907.
(37) Olmstead, M. H.; de Bettencourt-Dias, A.; Duchamp, J. C.; Stevenson, S.; Marciu, D.; Dorn, H. C.; Balch, A. L. *Angew. Chem., Int. Ed.* **2001**, *40*, 1223−1225.
(38) Olmstead, M. M.; Lee, H. M.; Duchamp, J. C.; Stevenson, S.; Marciu, D.; Dorn, H. C.; Balch, A. L. *Angew. Chem., Int. Ed.* **2003**, *42*, 900−902.
(39) Zuo, T. M.; Beavers, C. M.; Duchamp, J. C.; Campbell, A.; Dorn, H. C.; Olmstead, M. M.; Balch, A. L. *J. Am. Chem. Soc.* **2007**, *129*, 2035−2043.
(40) Beavers, C. M.; Chaur, M. N.; Olmstead, M. M.; Echegoyen, L.; Balch, A. L. *J. Am. Chem. Soc.* **2009**, *131*, 11519−11524.
(41) Lu, X.; Lian, Y.; Beavers, C. M.; Mizorogi, N.; Slanina, Z.; Nagase, S.; Akasaka, T. *J. Am. Chem. Soc.* **2011**, *133*, 10772−10775.
(42) Beavers, C. M.; Jin, H.; Yang, H.; Wang, Z. M.; Wang, X.; Ge, H.; Liu, Z.; Mercado, B. Q.; Olmstead, M. H.; Balch, A. L. *J. Am. Chem. Soc.* **2011**, *133*, 15338−15341.
(43) Yang, H.; Lu, C.; Liu, Z.; Jin, H.; Che, Y.; Olmstead, M. M.; Balch, A. L. *J. Am. Chem. Soc.* **2008**, *130*, 17296−17300.